HCR signal amplification strategy based photothermal sensing for histamine detection

Huiling Xue[a], Bing Zhang*[a], Ying Zhan[a], Zhihuan Zhao[a], Jianying Lin[a], Yan Cheng*[b,c]

a College of Chemistry and Chemical Engineering, Taiyuan University of Technology, Taiyuan 030024, China

b Department of Nuclear Medicine, First Hospital of Shanxi Medical University, Taiyuan 030001, China

c Collaborative Innovation Center for Molecular Imaging of Precision Medicine, Shanxi Medical University, Taiyuan, Shanxi, 030001, China.

Table S1 The respective sequences of the oligonucleotides used in this work.

oligonucleotide	sequence (from 5' to 3')
hDNA	UACGAUCCAGUGGGUUGAAGGAAAGUAACAGAUCGUA
tDNA	CCACTGGATCGTAT$_{10}$-NH$_2$
H1	TACGATCCAGTGGTACAAGCCACTGGA-SH
H2	CCACTGGATCGTATCCAGTGGCTTGTA-SH

* Corresponding author.
E-mail addresses: zhangbing01@tyut.edu.cn (B. Zhang).
* Corresponding author.
E-mail addresses: chengyan_1976@163.com (Y. Cheng).

Photothermal performance of CuS@Au nanocomposites

The CuS@Au dispersion was irradiated with an 808 nm near infrared (NIR) laser at a power density of 1.67 W cm^{-2} for 5 minutes, and the temperature profile was documented. After the laser was switched off, the cooling curve was monitored (Fig. S1A). The photothermal conversion efficiency (η) was computed using the following equation:

$$\eta = \frac{mc(T_{max} - T_{max,H_2O})}{I(1 - 10^{-A})\tau_s} \quad (1)$$

where A represents the absorbance of the CuS@Au at 808 nm, m denotes the mass of the solution, c is the specific heat capacity of water, I is the laser power density at 808 nm, T_{max} and $T_{max,\ H_2O}$ are the maximum temperatures of CuS@Au and water respectively, τ_s is the system time constant, which can be calculated according to the following formula:

$$t = -\tau_s \ln\left(\frac{T - T_{surr}}{T_{max} - T_{surr}}\right) = -\tau_s \ln(\theta) \quad (2)$$

where T is the temperature at time t, and Tsurr is the ambient temperature. The linear fitting of the cooling curve (Fig. S1B) resulted in the determination of τ_s. The calculated photothermal conversion efficiency (η) of the CuS@Au nanocomposites was 71.06%, suggesting their outstanding photothermal conversion ability. Moreover, the photothermal stability of CuS@Au was explored by subjecting the dispersion to three on-off cycles of NIR laser irradiation. As depicted in Fig. S1C, the temperature change remained consistent throughout all cycles, indicating the favorable photothermal stability of the nanomaterial.

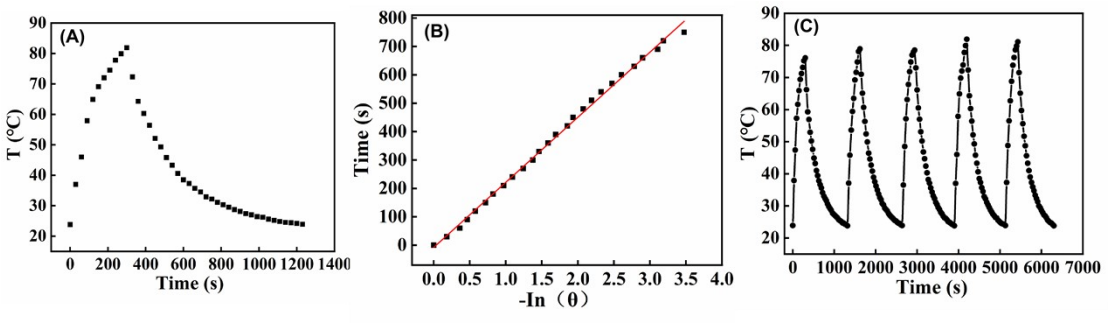

Fig. S1. (A) The temperature curve of the CuS@Au solution was irradiated with a laser at 808 nm; (B) Plot of heat transfer from the system of CuS@Au solution; and (C) The photothermal stability of CuS@Au solution.

Table S2 The comparison of the photothermal properties of different photothermal materials.

Potothermal Materials	Photothermal Conversion Efficiency (η)	Laser Wavelength	Power Density	Reference
CDs	54.3%	655nm	1.2 W cm^{-2}	1
MoS_2@Au	29.37%	808nm	3.15 W cm^{-2}	2
GCGLS	31%	808nm	1.5 W cm^{-2}	3
THPG vesicles	44.1%	635nm	0.2 W cm^{-2}	4
CCRZ NPs	39.8%	808nm	1.2 W cm^{-2}	5
GO-PANIZ-Ag0.125	44.4%	808nm	1.5 W cm^{-2}	6
CuS@Au	71.06%	808nm	1.67 W cm^{-2}	This work

Table S3 An overview for histamine detection by different method.

Detection methods	Materials	LOD	Linear range	Reference
FL	PF8BT-A	0.38 μM	3 - 21μM	7
SERS	Au NFs@ZIF-67	0.087 μM	0.1μM - 1mM	8
SERS	Au NPs	1.22 pM	10 pM - 1mM	9
Colorimetric	DCt-Au NPS	0.426 μM	1-100 μM	10
ECL	g-C_3N_4 NSs	0.043 μM	0.1 - 750 μM	11
photothermal	CuS@Au	0.82 pM	10 pM - 10 μM	This work

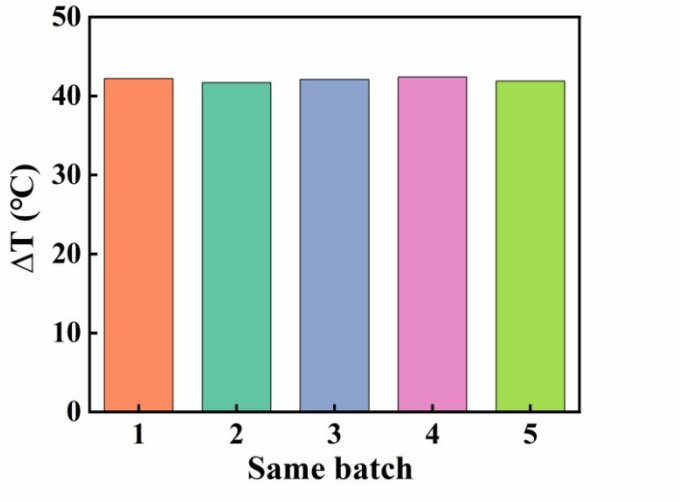

Fig. S2. Same batch of photothermal sensing.

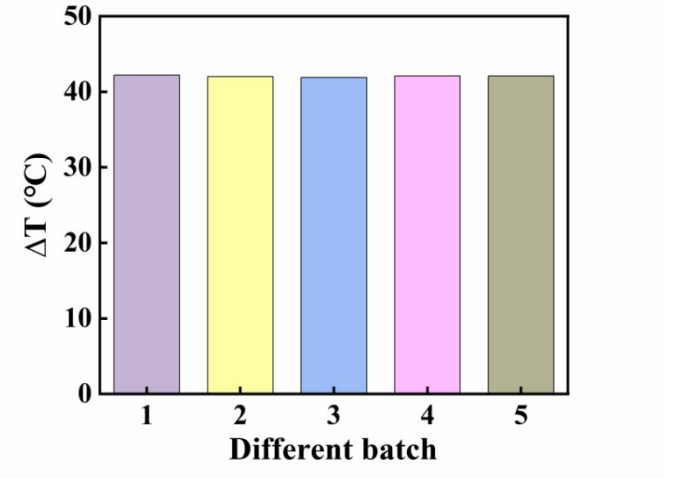

Fig. S3. Different batchesof photothermal sensing.

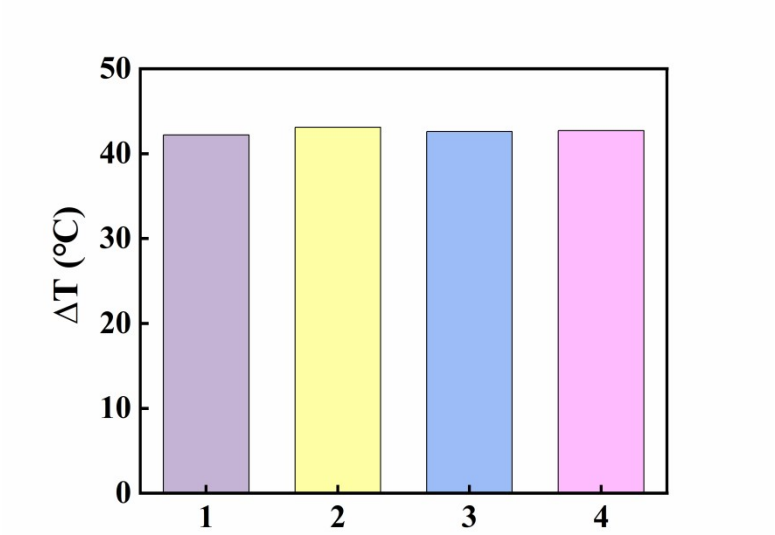

Fig. S4. Stability of photothermal sensing.

Table S4 Comparison of the results for food samples by using the developed photothermal sensing and GB 5009.208-2016.

Sample	GB 5009.208-2016 (mean±SD, μM)	photothermal (mean±SD, μM)	t_{exp}
Fish	2.8172 ± 0.0023	2.9303 ± 0.216	-0.7404
	5.9015 ± 0.0152	6.5097 ± 0.292	-2.9416
	9.5493 ± 0.0017	9.5243 ± 0.216	0.1636
Shrimp	2.9090 ± 0.0077	3.0497 ± 0.147	-1.3517
	5.7927 ± 0.0115	6.12167 ± 0.216	-2.1508
	9.3338 ± 0.0021	9.3917 ± 0.083	-0.9862

References

1. Permatasari F A, Fukazawa H, Ogi T, Iskandar F, Okuyama K, Design of pyrrolic-N-rich carbon dots with absorption in the first near-infrared window for photothermal therapy, ACS Appl Nano Mater, 2018, 1, 2368-2375.

2. Lu L X, Ge Y Y, Wang X, Lu Z, Wang T, Zhang H Y, Du S Y, Rapid and sensitive multimode detection of Salmonella typhimurium based on the photothermal effect and peroxidase-like activity of MoS2@ Au nanocomposite, Sens Actuators B Chem, 2021, 326, 128807.

3. Zou Y B, Jin H L, Sun F, Dai X M, Xu Z S, Yang S L, Liao G F, Design and synthesis of a lead sulfide based nanotheranostic agent for computer tomography/magnetic resonance dual-mode-bioimaging-guided photothermal therapy, ACS Appl Nano Mater, 2018, 1, 2294-2305.

4. Liu Y N, Wang H, Li S L, Chen C S, Xu L, Huang P, Liu F, Su Y, Qi M W, Yu C Y, Zhou Y F, In situ supramolecular polymerization-enhanced self-assembly of polymer vesicles for highly efficient photothermal therapy, Nat Commun, 2020, 11, 1724.

5. Yang Z X, Liu Y, Wang J, Li W Z, Song P, Zhu L B, Zhang W W, Gui L, Ge F, Construction of pH-Responsive Copper Sulfide Nanocomposites and Their Photothermal/Chemodynamic Synergistic Antibacterial Studies, ACS Appl Nano Mater, 2025, 8, 8037-8053.

6. Bayar E Y, GETİREN B, Soysal F, Ciplak Z, Yildiz N, Bayraktar E, Graphene oxide/polyaniline/silver nanocomposite synthesis and photothermal performance, Mater Res Bull, 2023, 166, 112352.

7. Wu G, Ding Z Y, Dou X L, Chen Z, Xie J, Recognition and detection of histamine in foods using aptamer modified fluorescence polymer dots sensors, Spectrochim Acta A, 2024, 317, 124452.

8. Xu S, Chen P F, Lin X C, Khan I M, Ma X Y, Wang Z P, Controllable synthesis of flower-like AuNFs@ ZIF-67 core-shell nanocomposites for ultrasensitive SERS detection of histamine in fish, Anal Chim Acta, 2023, 1240, 340776.

9. Wang B H, Jiang H, Tang R Y, Tan Y Y, Xia X M, Zhang X, Construction of histamine aptamer sensor based on Au NPs nanozyme for ultrasensitive SERS detection of histamine, J Food Compos Anal, 2023, 120, 105337.

10. Unabia R B, Reazo R L D, Rivera R B P, Lapening M A, Omping J L, Lumod R M, Ruda A G, Dopamine-functionalized gold nanoparticles for colorimetric detection of histamine, ACS Omega, 2024, 9, 17238-17246.

11. Mesgari F, Salehnia F, Beigi S M, Hosseini M, Ganjali M R, Enzyme free electrochemiluminescence sensor of histamine based on graphite-carbon nitride nanosheets, Electroanal, 2022, 34, 659-666.